Nonlinear Dynamics and Neuroscience

Izvestiya Vysshikh Uchebnykh Zavedeniy. Applied Nonlinear Dynamics. 2023;31(3)

Article DOI: 10.18500/0869-6632-003036

Ambient light at night causes desynchronization of rhythms in the sleep–wake switching model

K. O. Merkulova✉, *D. E. Postnov*

Saratov State University, Russia
E-mail: ✉merksenia@gmail.com, postnov@info.sgu.ru

Received 9.02.2023, accepted 17.03.2023, available online 7.04.2023, published 31.05.2023

Abstract. *The purpose* of this study is to analyze the influence of the shape of the daily illumination profile on the synchronization of rhythms in the sleep–wake state switching model. Normally, the alternation of sleep and wakefulness of a person is synchronized with his circadian rhythm and with the 24-hour rhythm of illumination. There is, however, a lot of experimental evidence of a violation of this synchronism, both in the form of phase failures (for example, during air travel) and in the form of long-term mismatch of rhythms (for example, during shift work in production). Mathematical models of the process of switching between sleep and wakefulness also demonstrate the desynchronization of rhythms and are successfully used to optimize work schedules. At the same time, the influence of a number of factors on this process has not been sufficiently studied, including the nature of changes in illumination during the day. *Methods.* An analysis of the six-dimensional model under study shows that, in terms of nonlinear dynamics, the problem is reduced to finding and interpreting resonance regions on a three-dimensional torus. For the specific purposes of our work, it turned out to be convenient to estimate the ratio of three periods (24 hours, the circadian period, and the current duration of the sleep–wake cycle) by numerically integrating the model equations on a grid of parameter values using parallel computing technology. *The main result* of our work is that the presence of round-the-clock low-intensity illumination (that is, the addition of a zero-frequency signal to the daily light cycle) causes the circadian rhythm to desynchronize with respect to the daily one in a significant range of parameters. We have proposed an explanation of this effect based on the structure of the mathematical model. *Conclusion.* Our results raise at least two serious questions, the first of which is related to the physiological interpretation of one of the main variables of the model, sleep homeostasis, and the second is to refine the assumptions that are used in the model description of the photoreceptor response. In any case, there are interesting prospects for further research.

Keywords: sleep–wake cycle, circadian rhythm, desynchronization, mathematical model.

Acknowledgements. This work was supported by Russian Foundation for Basic Research, grant No. 22-15-00143.

For citation: Merkulova KO, Postnov DE. Ambient light at night causes desynchronization of rhythms in the sleep–wake switching model. Izvestiya VUZ. Applied Nonlinear Dynamics. 2023;31(3):351–364. DOI: 10.18500/0869-6632-003036

Introduction

In 1982, A.A. Borbeli published the first mathematical model of regulation of the sleep-wake process [1]. It is known as the «two-process model», later supplemented in the works [2–6].

The first of the two processes is sleep homeostasis. It reflects the need for sleep, which increases during wakefulness and decreases during sleep [1].

The second process is the circadian process. It is synchronized with the circadian rhythm and affects the sequence of episodes of sleep and wakefulness. It promotes wakefulness, counteracts the homeostatic need for daytime sleep and is responsible for consolidating sleep episodes at night [1, 7].

In the mathematical models mentioned above, two processes correspond to two self-oscillating subsystems («oscillators»), which are influenced by the time of day, behavioral characteristics, nutrition rhythm, physical activity level and other environmental factors (Zeitgeber). The main factor is the rhythm of alternating light and darkness [7–9].

Disruptions in the light rhythm can occur during air travel, during shift work in production, in the service sector, in medicine. Their influence on the condition of employees is extremely important and therefore has become the subject of intensive study: experimental [10–13] and model [14, 15].

The above factors and other unidentified causes may cause a violation of synchronism between the circadian rhythm and the sleep-wake cycle [16–18]. With such disorders, it is difficult (sometimes impossible) for a person to maintain a socially normal daily routine and work schedule. This aggravates the situation with sleep and health [19]. These problems are attributed to disturbances in the circadian rhythm system, but their exact mechanisms are unknown [20].

The influence of light rhythm phase failures in the above-mentioned works has been well studied. Less attention is currently paid to non-explicit and more difficult to control characteristics (for example, the illumination profile during the day). In relation to a single circadian rhythm , this problem was solved [7, 21]. However, the role of diurnal changes in illumination in the desynchronization of all three rhythms has not been practically investigated.

In this study, we rely on a specific version of the mathematical model of neural populations (neuron mass models) proposed in [22]. Like many other system-level models, it was originally built with the aim of the best quantitative description of experimentally recorded patterns in the language of the level of activity and the nature of the interaction of physiologically significant blocks — neural nuclei. Thus, in the work [23] it is shown that a similar type of model, based on the model of Jansen and Rita, can generate multi-frequency rhythms that are close to real EEG rhythms. And the model presented in [24] is capable of reproducing EEG data for sleep stages N2 and N3 with high accuracy. The choice of a specific model for our research is due to the fact that it relies on recent developments of models of this type [25, 26] and reproduces experimental data on the occurrence of the effect of desynchronization between the rhythms of the body and the circadian rhythm (spontaneous internal desynchrony, SID). In the work [22] it is shown that the type of nonlinearity used and the selected parameter values provide better compliance with laboratory studies compared to prototype models.

During the computational experiment, we construct two-parameter diagrams of the values of the periods of the two rhythms of the model and analyze the obtained dependencies at different levels of background illumination. The main result of our analysis is that the presence of night illumination weakly changes the modes in the region of typical parameter selection, but causes significant changes in the adjacent area of the diagram and may be an important factor in the synchronization of the studied rhythms. We offer an explanation of the results obtained based on the analysis of the features of the relationship of the model equations, and also discuss the questions arising in this case on the topic of physiological interpretation of variables and parameters of the model.

1. Methodology

1.1. Model. In this section we briefly describe the model, which is justified in detail in the work [22]. In this and other similar models, the processes are described in terms of populations of neurons and their interactions. The block diagram of the model is shown in Fig. 1 and includes a photoreceptor activation unit (1), a circadian oscillator (2), neural core switching units (3) and (4), a block sleep

homeostasis (5) and state-dependent (sleep or wake) connections of elements (6).

Physiologically, the state of sleep or wake is determined by the work of the neural nuclei of the brain: MA (monoaminergic nuclei, the center of wake) and VLPO (ventrolateral preoptic nucleus of the hypothalamus, the center of sleep). The activity of these nuclei is described by the average voltage of the populations of neurons: for the sleep center, this is the variable V_v, and for the wake center — V_m. The wake state is registered when V_m exceeds the predefined threshold value V_{th}. Otherwise, it is assumed that the system is in a state of sleep. VLPO and MA cores (blocks 3 and 4 in Fig. 1) are interconnected by inhibitory bonds and form a bistable system that, in the absence of external influence, can remain in one of two stable states for a long time. Changing states (switching the activity of cores) it is caused by circadian and homeostatic processes affecting them (modules 2 and 5 in Fig. 1). The activity of the nuclei is also affected by their lateral connections (signals from other populations of neurons), which in this version of the model are extremely simplified by the control parameters A_v and A_m presented.

The activity level of the nucleus is defined as the average frequency of neuronal excitation $Q(V_i)$ and is described by the sigmoid function of the average voltage of the corresponding population V_i

$$Q(V_i) = \frac{Q_{\max}}{1 + e^{(\Theta - V_i)/\sigma'}}, \quad i = m, v, \tag{1}$$

where $Q_{\max}$ is the maximum possible pulse generation frequency, Θ is the average action potential of a neuron relative to rest, and $\sigma'\pi/\sqrt{3}$ is its standard deviation [25].

The equations describing the activity of the MA and VLPO nuclei have the form:

$$\tau_v \frac{dV_v}{dt} = \nu_{vm} Q(V_m) - V_v + A_v + \nu_{vH} H + \nu_{vC} C(X, Y), \tag{2}$$

$$\tau_m \frac{dV_m}{dt} = \nu_{mv} Q(V_v) - V_m + A_m, \tag{3}$$

where τ_v and τ_m — time constants, v_{mv} and v_{vm} — parameters of the influence of nuclei on each other, A_v and A_m — the parameters mentioned above, representing inputs from other populations of neurons. The terms $\nu_{vH} H$ and $\nu_{vC} C(X, Y)$ describe the effects of the homeostatic and circadian process.

The homeostatic process H (block 5) is completely determined by the activity of the wake center $\mathrm{Q}(V_m)$. It is described by the equation:

$$\tau_H \frac{dH}{dt} = \nu_{Hm} Q(V_m) - H, \tag{4}$$

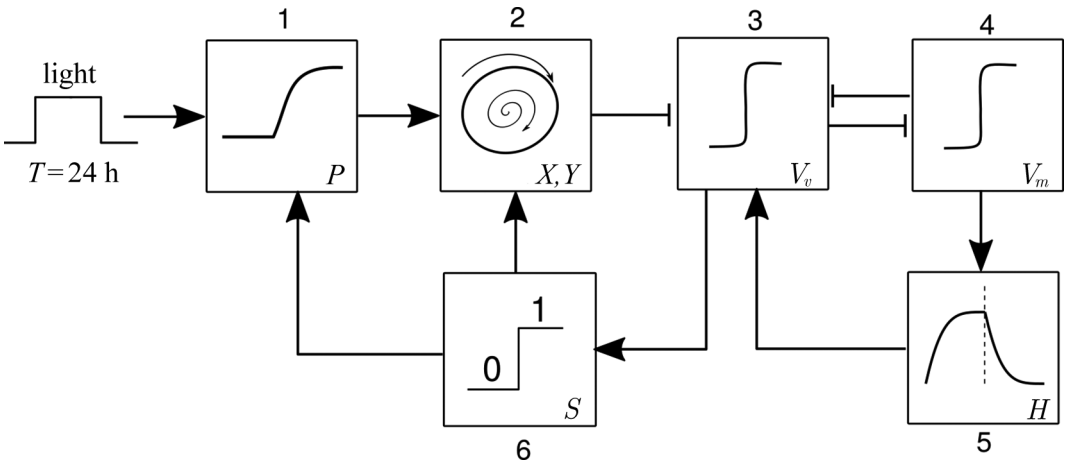

Fig. 1. The structure of the mathematical model: 1 — the level of photoreceptor activation (variable P) depends on the incoming light and the current state of the system S; 2 — circadian rhythm generator (variables X, Y); 3 — "sleep center", ventrolateral preoptic nucleus of the hypothalamus (VLPO), variable V_v; 4 — "wake center", monoaminergic nuclei (MA), variable V_m; 5 — homeostatic process, variable H; 6 — threshold filtering procedure maps sleep and wake states to $S = 0$ and $S = 1$, respectively

where τ_H is the time constant of the homeostatic process, and ν_{Hm} sets the impact force from MA.

The circadian process C (block 2) has the form of quasi-harmonic oscillations and is generated by an self-oscillatory subsystem of two equations for the variables X and Y

$$\tau_x \frac{dX}{dt} = Y + \gamma\left(\frac{1}{3}X + \frac{4}{3}X^3 - \frac{256}{105}X^7\right) + C_{Xn} + C_{Xp}, \tag{5}$$

$$\tau_y \frac{dY}{dt} = -\left(\frac{\delta}{\tau_c}\right)^2 X + C_{Yp}, \tag{6}$$

where τ_x, τ_y — time constants that set the period of the oscillator, γ — parameter controlling the shape of the oscillations, τ_c and δ — parameters entered to coordinate with experimental data [27]. A specific form of the nonlinear function $C(X, Y)$ is proposed in [22] to better match the experimental data.

Empirically selected nonlinear functions C_{Xp}, C_{Yp} and C_{Xn} determine the influence of light and other environmental factors that attract biological rhythms to a 24-hour daily rhythm.

The effect of the circadian oscillator on the activity of the VLPO core is given in the equation (2) using the function

$$C(X, Y) = 0.1\frac{(X+1)}{2} + \left(\frac{c_1 X - c_2 Y + c_3}{X+2}\right)^2, \tag{7}$$

where the strength of the circadian effect is expressed by the parameter v_{vC}, and the shape is regulated by the parameters c_1, c_2 and c_3.

The light -independent effects on the circadian oscillator by the homeostatic oscillator are given by the following relations:

$$C_{Xn} = \nu_{Xn}\left(\frac{1}{3} - (1 - S)\right)(1 - \tanh(rX)), \tag{8}$$

$$S = U(V_m - V_{\text{th}}), \tag{9}$$

where ν_{Xn} is a parameter characterizing the coupling strength of factors unrelated to light, and the constant r makes the effect dependent on the phase of the circadian oscillator. The system state function S is expressed in terms of a step function U, which takes a single value when $V_m - V_{\text{th}} > 0$ (the system «does not sleep»), or zero, when $V_m - V_{\text{th}} \leqslant 0$ (the system «sleeps»).

The light-dependent effect on the circadian oscillator is set using the functions C_{Xp} and C_{Yp} for each of the oscillator variables

$$C_{Xp} = \nu_{Xp}\alpha_I(1 - P)(1 - \varepsilon X)(1 - \varepsilon Y), \tag{10}$$

$$C_{Yp} = \alpha_I(1 - P)(1 - \varepsilon X)(1 - \varepsilon Y)(\nu_{YY}Y - \nu_{YX}X). \tag{11}$$

The parameters ν_{YY} and ν_{YX} make the effect dependent on the current phase of the circadian oscillator, and ε sets the degree of sensitivity of the light component to circadian variables.

Physiologically, the effect of light on the circadian system is carried out through ganglial cells (photoreceptors) on the retina of the eyes [28, 29]. In the model, the activity of photoreceptors is represented by the variable P and is expressed by the following equations:

$$\tau_P \frac{P}{dt} = \alpha_I(1 - P) - \beta P, \tag{12}$$

$$\alpha_I = \alpha_0 S \frac{I(t)}{I(t) + I_1}\sqrt{\frac{I(t)}{I_0}}. \tag{13}$$

The proportion of photoreceptors ready for activation is $(1 - P)$. They become active at the rate of α_I and are spontaneously deactivated at the rate of β. The parameters α_0, I_0, I_1 set the dependence of photoreceptor activity on the current light intensity $I(t)$, τ_p — activation time constant. The presence of the state of the system S in the equation (13) makes the light signal significant only in the wake state (eyes are open).

1.2. Light profile. The daily illumination profile $I(t)$ in real conditions can have a variety of forms depending on geographical latitude, weather events, etc. In an urban environment, it is largely determined by social factors (work schedule). Taking into account artificial lighting, it can be presented in the form of a sequential change of day and night lighting. This corresponds to a signal of the type «meander» (Fig. 2). Control parameters of the model I_{amb} and I_{ext} set the level of background illumination and the scope of the main signal. It can be seen from the figure that the presence of background illumination raises the entire signal, but does not change its shape, and increases the amplitude of the constant component in the spectrum. But such changes can dramatically change the dynamic mode of the system as a whole.

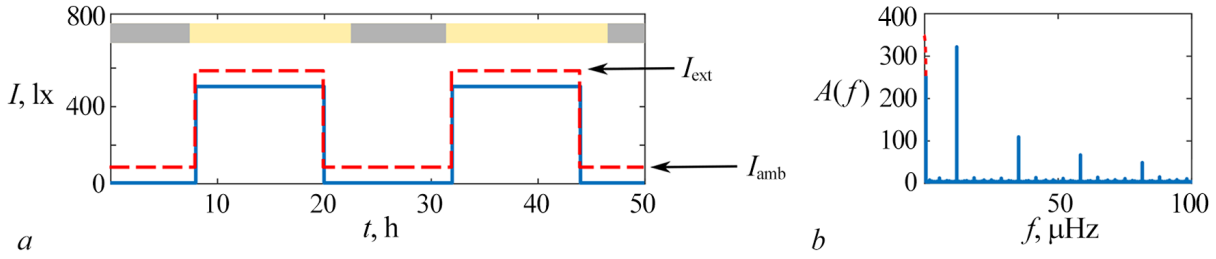

Fig. 2. Light diurnal profile in the form of a meander with a peak intensity $I_{\text{ext}} = 500$ lx (a) and its amplitude Fourier spectrum (b). The red dotted line illustrates the changes in the presence of background illumination with an intensity $I_{\text{amb}} = 100$ lx. The bar at the top of the panel shows the transition between sleep (gray) and wakefulness (yellow) for a typical choice of control parameters (color online)

1.3. Computational method. To estimate the period of each of the two internal rhythms of the system, its numerical integration was performed with the same initial conditions, but different combinations of control parameters. It was believed that the establishment period takes no more than 1000 hours of model time. In the next 1000 hours, the average values of the period of the circadian oscillator T_{c} for the temporary realization of the variable X and the period of the sleep-wake rhythm T_{s} for the temporary realization of the variable V_m were calculated. This procedure was performed independently for each combination of control parameters τ_H and I_{ext}. To speed up calculations, all combinations of parameters were processed simultaneously using the parallel computing method on GPUs. The analysis of the current regime was based on the ratio of the periods of three rhythms: the daily rhythm with a period of strictly 24 hours, the circadian rhythm with a period of T_{c} and the homeostatic rhythm with a period of T_{s}.

Two different programs were used to integrate the equations. The first (in the Octave environment using the lsode function and double-precision variables) was considered the reference. The second program (in the NVIDIA CUDA development environment) was used to calculate two-parameter diagrams. It used a variation of the 4-order Runge-Kutta method with a fixed step ($h = 0.001$ h), adapted for solving both ordinary and stochastic differential equations [30–32]. There were no significant discrepancies in the calculation results of the two programs indicated.

1.4. Values of control parameters. We relied on a set of control parameters from [22]. The main part of them was selected from the point of view of quantitative compliance with experimental data. We considered them constants. Freely variable parameters can be considered the parameters of the intensity of light exposure I_{amb}, I_{ext}, as well as the parameter τ_H. Its physiological meaning and role in the model are clear, but a reasonable quantitative assessment is difficult. Below are the values of those parameters that were considered constants: $Q_{\max} = 100$ Hz; $\Theta = 10$ mV; $\sigma' = 3$ mV; $\tau_v = \tau_m = 50/3600$ h; $\nu_{vm} = -2.1/3600$ mV·h; $\nu_{mv} = -1.8/3600$ mV·h; $A_v = -10.3$ mV; $A_m = 1.3$ mV; $V_{\text{th}} = -2$ mV; $\nu_{vH} = 1$ mV; $\nu_{vC} = -0.5$ mV; $\tau_H = 59$ h; $\nu_{Hm} = 4.57/3600$ h; $\tau_x = \tau_y = 24/(2\pi)$ h; $\gamma = 0.13$;

$\tau_c = 24.2$ h; $\delta = 24.2/0.99729$ h; $c_1 = 0.838$; $c_2 = 0.676$; $c_3 = 1.136$; $\nu_{Xn} = 0.032$; $r = 10$ h; $\nu_{Xp} = 37$; $\nu_{YY} = 12.33/60$ h; $\nu_{YX} = 20.35/60$ h; $\varepsilon = 0.4$; $\beta = 0.007/60$ Hz; $\alpha_0 = 0.1/60$ Hz; $I_0 = 9500$ lx; $I_1 = 100$ lx; $\tau_p = 1/3600$ h.

2. Results

When studying the dynamics of the sleep-wake cycle, it is customary to present the results of calculations or measurements in the form of diagrams. In Fig. 3, *a* and *b* time is deferred on both axes, in hours horizontally and days vertically.

Alternating periods of sleep and wakefulness are highlighted with a color fill. Red and green labels indicate the position of the main biological markers: the minimum internal body temperature (green triangles) and the peak of melatonin in plasma (red squares). Using such diagrams, it is easy to diagnose the absence (panel *a*) or the presence (panel *b*) of synchronicity of processes in relation to the circadian rhythm. The horizontal shift and «jump» of zones and markers is clearly visible on the *a* panel.

In this paper, we use a more traditional approach: we compare the periods of two self-oscillating subsystems of the model calculated over a sufficiently long period of time. In Fig. 3, *c* such dependencies

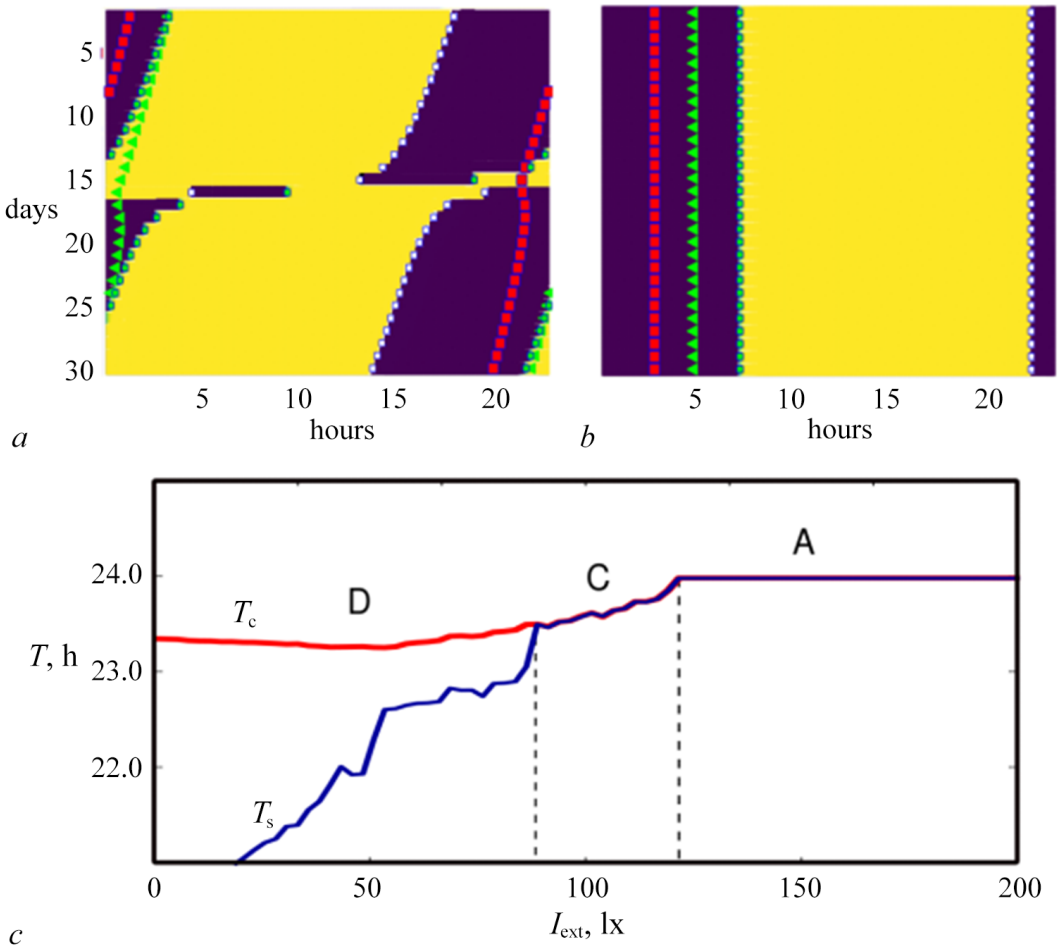

Fig. 3. *a, b* — Representation of the model dynamics in the form of daily diagrams in the absence of constant illumination and various levels of daylight illumination I_{ext}: 10 lx (*a*), 200 lx (*b*). The values of other parameters are given in the section 1.4. Purple shading corresponds to sleep intervals, yellow — to waking intervals. Red markers show the phase of the circadian rhythm. Panel *c* is single parameter diagram of dependence of the periods of the circadian rhythm (T_c) and the sleep–wake cycle (T_s) on the degree of daylight I_{ext} at $\tau_H = 58.0$ (color online)

are given for $\tau_H = 58.0$. In the right part of the graph (letter A), both curves coincide and lie at the level of 24 hours. That is, both internal rhythms of the system are synchronized with the light circadian rhythm, $T_s = T_c = 24.0$ hours. This is a physiologically normal mode, which is implemented with a typical choice of parameters. At lower light levels, in the region C, both periods are different from the daily period of 24 hours, but synchronized with each other, $T_c = T_s$. Finally, in the region D, at low levels of daylight intensity I_{ext}, all three periods are different, $T_c = 23.2 \ldots 23.5$ hours, and T_s decreases with decreasing I_{ext}.

In Fig. 4 the values of the circadian period T_c are given already on the plane of two control parameters τ_H and I_{ext} for different values of background illumination I_{amb}. The analysis of such diagrams allows us to identify three modes (regions A, C, D) and another mode (region B), where the period of the circadian rhythm is T_c within the accuracy of calculations, it is equal to 24.0 hours, and T_s has significantly lower values, about 18 hours.

The splitting of the parameter plane described above has a clear interpretation from the point of view of synchronization theory [33, 34]. So, the region A corresponds to the main region ($24 : T_c : T_s = 1 : 1 : 1$) of synchronization of three rhythms, where the values of all three periods are the same. The regions B and C are partial synchronization zones where 2 of the 3 frequencies coincide, and the resulting oscillatory mode is two-frequency quasi-periodic oscillations. The region D corresponds to a completely non-synchronous behavior when all three rhythms have different periods. In the work [35], a similar hierarchy of the degree of synchronicity is shown by the example of the simplest model system. In the framework of this work, we do not consider resonances of the form $(1 : 1 : n)$, $n = 1, 2, 3..$, which are located in the region $\tau_H < 50$. In this study, we are interested in the region B, or rather, the effect we found of its disappearance with an increase in the intensity of the background illumination I_{amb}.

Panel *a* fig. 4 corresponds to fig. 3. but for better visualization, a different vertical scale is selected for the value T_c, from 23 to 24.5 hours. At the same time, the values of T_s in the region B and D are not displayed, but the behavior of T_c can be seen in more detail. The intensity of the background illumination I_{amb} in Fig. 4 increases from top to bottom and is 0, 25 and 50 lx for panels *a*, *b* and *c*. Comparing panels allows you to see the influence of background illumination in dynamics: with its increase, numerous zones of weak resonances and transitions between them are smoothed out, the area of full synchronization A decreases in size, but most importantly — at $I_{amb} = 50$ lx (*c*) completely disappears region B! Thus, the addition of a constant component, that is, a zero-frequency signal, significantly affects the picture of the interaction of the three rhythms in the system under study.

The high sensitivity of the process of switching between sleep and wakefulness to excessive lighting at night is known to physiologists and has been studied experimentally [36].

For additional information, one-parameter dependences of the values T_c and T_s on the intensity of daylight I_{ext} were constructed (Fig. 5).

The dependence of T_s on I_{ext} changes little in the presence of background illumination, there is no unambiguous trend. At the same time, the graph for T_c, in all cases located between T_s and the value of 24 hours, monotonically shifts towards T_s. The black, blue and red curves correspond to the background illumination of I_{amb} at 0, 25 and 50 lx, respectively. This can be interpreted in two ways: either as a weakening of the synchronizing action on the part of the 24-hour rhythm, or as an increase in the action on the part of the sleep-wake rhythm.

The task of this work was to offer a nonlinear-dynamic, rather than a physiological explanation of the effects found. Therefore, in his search, the features of the model equations (1)–(13) were analyzed, which can lead to the effects we found.

The first hypothesis tested was related to the possible contribution of the nonlinear photoreceptor activation function (13). It turned out that in the studied range of parameter values, the presence of background illumination is very insignificant (less than 5%) and changes the ratio of the amplitudes of the constant component and the amplitudes of harmonics in the spectrum of the signal converted according to (13). Additional calculations, in which various waveforms were tested, showed that the structure of the diagrams rather weakly depends on the change in the ratio of the amplitudes of their harmonics.

However, testing of various forms of the daytime profile suggested a possible mechanism of action of background illumination, which manifests itself most strongly for a signal in the form of a meander. In Fig. 2 at the top of the panel *a* color gradation shows the change of waking states (yellow) and sleep

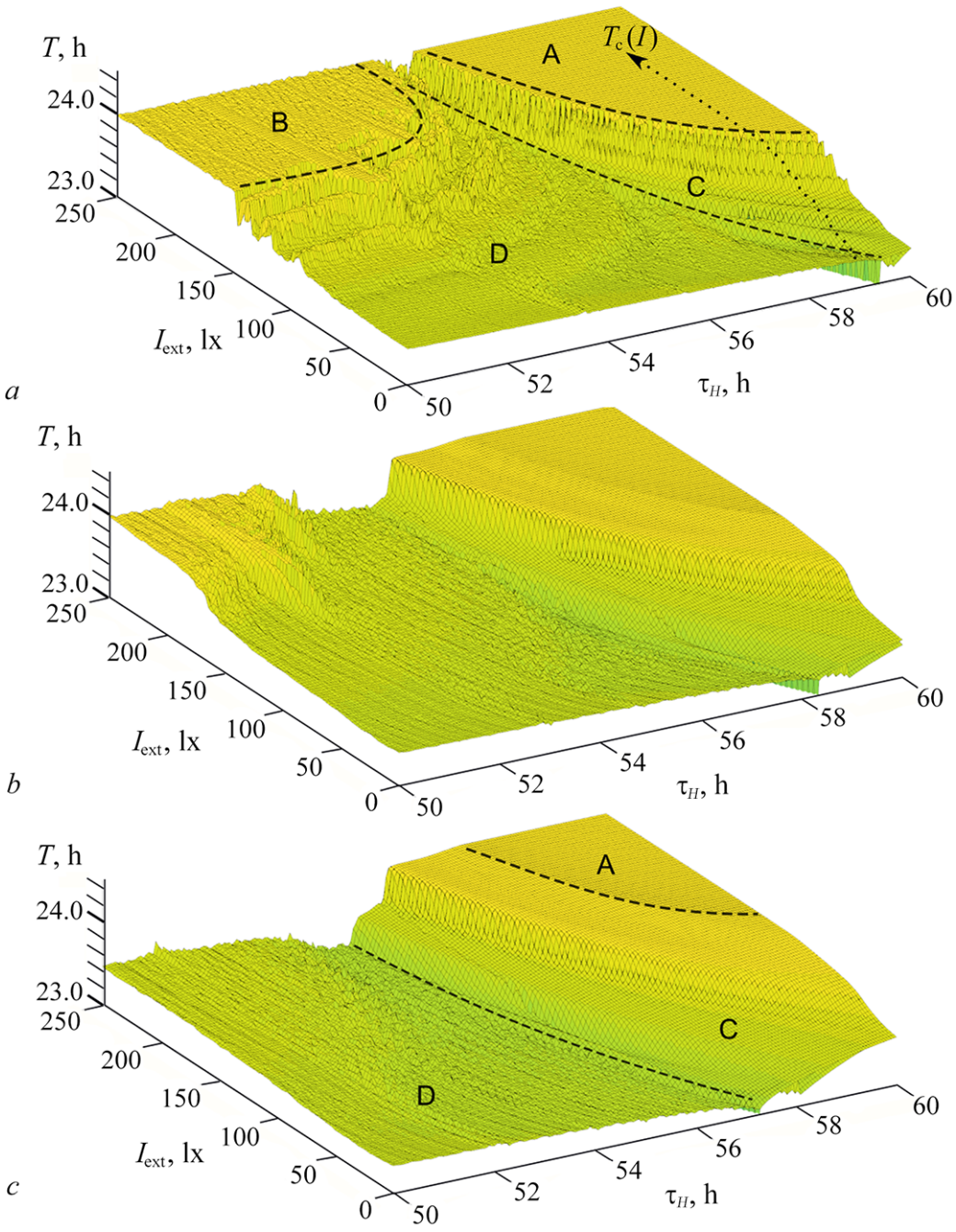

Fig. 4. The values of the circadian period T_c on the plane of the control parameters τ_H and I_{ext} for different values of the background illumination intensity $I_{amb} = 0, 25, 50$ lx for panels *a*, *b* and *c* respectively. Dashed lines and letters A, B, C, D delimit the regions of modes of varying degrees of synchronicity, see text (color online)

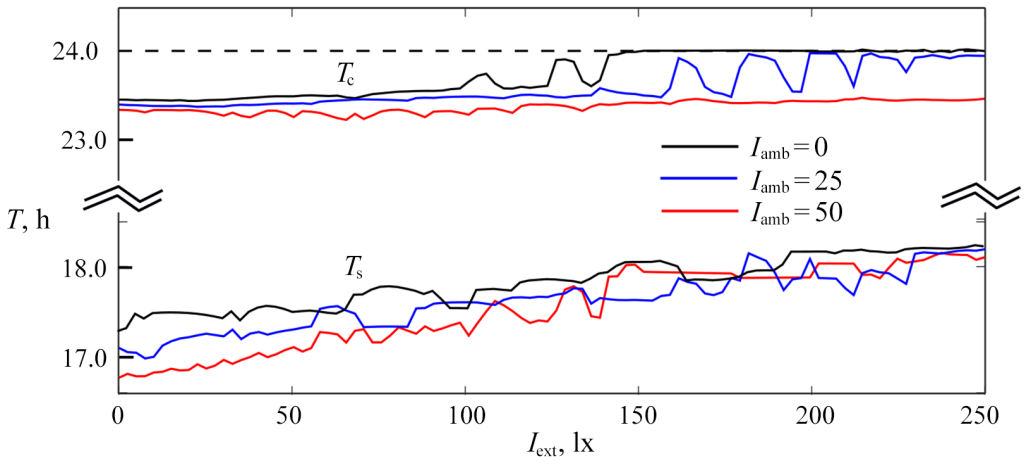

Fig. 5. Dependence of T_c and T_s on daylight intensity I_{ext} for $\tau_H = 52.0$ (color online)

(gray) for the region A in Fig. 4. In the expression (13), this dependence is included as a multiplication by the current state of the system S. The phases of the signals correspond to a typical steady-state mode. In the absence of illumination (blue curve) during sleep, when $S = 0$, the light signal is also zero, and their multiplication in the expression (13) does not change either the shape or the spectral composition of the effect on the circadian oscillator. In the presence of night illumination, its multiplication with S generates an oscillatory component α_I, which in frequency and phase duplicates the process of switching between sleep and wakefulness. This is qualitatively equivalent to an increase in the degree of influence on the circadian oscillator, originally laid down in the ratio (8). As the background illumination of I_{amb} increases, this additional synchronizing effect on T_c increases and counteracts the synchronization of the circadian rhythm with the daily one.

Additional calculations with various forms of the light profile confirmed that the region of partial synchronization B decreases or disappears altogether for those signals that have a region of non-zero values during sleep periods. The exclusion of the value S from the ratio (13) significantly expands the area of synchronicity of the circadian rhythm with the daily 24-hour cycle and significantly weakens its dependence on the parameter τ_H.

Conclusion

We investigated how the shape of the light profile signal affects the synchronicity of the daily 24-hour cycle, circadian rhythm and the process of changing sleep-wake states in a mathematical model that was previously published in [22] as the most accurately reproducing experimental data.

The main result of our work is that the presence of low-intensity illumination around the clock (the addition of a zero-frequency signal to the signal of the daily light cycle) causes a desynchronization of the circadian rhythm relative to the daily one in a significant range of parameters. An increase in the intensity of background illumination (from 0 to 50 lx) leads to a decrease in size and complete disappearance of the partially synchronous mode area, within which the circadian rhythm is synchronized with the daily 24-hour rhythm.

We have proposed an explanation of this effect based on the structure of a mathematical model. This effect of night illumination is a consequence of the assumption that photoreceptors are insensitive to light during sleep. Mathematically, this is implemented as strobing the light signal with the sleep-wake rhythm, therefore, in certain situations it leads to a mode competition type effect — the amplification of the action of the homeostatic oscillator is not able to synchronize the circadian oscillator, but it is enough to «detach» circadian oscillations from the 24-hour daily cycle.

Our results raise at least two serious questions. The first question is related to the physiological

interpretation of sleep homeostasis, or rather, to the additional justification of the parameter τ_H, which turns out to be critically important for synchronizing rhythms, as we have already noted in [37]. The second question is related to clarifying the assumptions used in the model description of the reaction of photoreceptors. The assumption of their complete insensitivity to light during sleep is a strong simplification of the situation. In any case, there are interesting prospects for further improvement of the model.

References

1. Borbély AA. A two process model of sleep regulation. Hum. Neurobiol. 1982;1(3):195–204.
2. Achermann P, Borbély AA. Simulation of human sleep: ultradian dynamics of electroencephalographic slow-wave activity. Journal of Biological Rhythms. 1990;5(2):141–157. DOI: 10.1177/074873049000500206.
3. Achermann P, Borbély AA. Simulation of daytime vigilance by the additive interaction of a homeostatic and a circadian process. Biological Cybernetics. 1994;71(2):115–121. DOI: 10.1007/BF00197314.
4. Achermann P, Dijk DJ, Brunner DP, Borbély AA. A model of human sleep homeostasis based on EEG slow-wave activity: Quantitative comparison of data and simulations. Brain Research Bulletin. 1993;31(1–2):97–113. DOI: 10.1016/0361-9230(93)90016-5.
5. Achermann P. The two-process model of sleep regulation revisited. Aviation, Space, and Environmental Medicine. 2004;75(Suppl 3):LA37–A43.
6. Borbély AA, Daan S, Wirz-Justice A, Deboer T. The two-process model of sleep regulation: a reappraisal. Journal of Sleep Research. 2016;25(2):131–143. DOI: 10.1111/jsr.12371.
7. Golombek DA, Rosenstein RE. Physiology of circadian entrainment. Physiol. Rev. 2010; 90(3): 1063–1102. DOI: 10.1152/physrev.00009.2009.
8. Kalsbeek A, la Fleur S, Fliers E. Circadian control of glucose metabolism. Molecular Metabolism. 2014;3(4):372–383. DOI: 10.1016/j.molmet.2014.03.002.
9. Youngstedt SD, Elliott JA, Kripke DF. Human circadian phase–response curves for exercise. The Journal of Physiology. 2019;597(8):2253–2268. DOI: 10.1113/JP276943.
10. Casjens S, Brenscheidt F, Tisch A, Beermann B, Brüning T, Behrens T, Rabstein S. Social jetlag and sleep debts are altered in different rosters of night shift work. PLoS ONE. 2022;17(1):e0262049. DOI: 10.1371/journal.pone.0262049.
11. Hulsegge G, Loef B, van Kerkhof LW, Roenneberg T, van der Beek AJ, Proper KI. Shift work, sleep disturbances and social jetlag in healthcare workers. Journal of Sleep Research. 2019;28(4):e12802. DOI: 10.1111/jsr.12802.
12. Sűdy ÁR, Ella K, Bódizs R, Káldi K. Association of social jetlag with sleep quality and autonomic cardiac control during sleep in young healthy men. Front. Neurosci. 2019;13:950. DOI: 10.3389/fnins.2019.00950.
13. Deacon S, Arendt J. Adapting to phase shifts, I. An experimental model for jet lag and shift work. Physiology & Behavior. 1996;59(4–5):665–673. DOI: 10.1016/0031-9384(95)02147-7.
14. Skeldon AC, Phillips AJK, Dijk DJ. The effects of self-selected light-dark cycles and social constraints on human sleep and circadian timing: a modeling approach. Scientific Reports. 2017;7(1):45158. DOI: 10.1038/srep45158.
15. Putilov AA, Verevkin EG. Simulation of the ontogeny of social jet lag: A shift in just one of the parameters of a model of sleep-wake regulating process accounts for the delay of sleep phase across adolescence. Front. Physiol. 2018;9:1529. DOI: 10.3389/fphys.2018.01529.
16. Harvey AG. Sleep and circadian rhythms in bipolar disorder: Seeking synchrony, harmony, and regulation. The American Journal of Psychiatry. 2008;165(7):820–829. DOI: 10.1176/appi.ajp. 2008.08010098.
17. Hickie IB, Naismith SL, Robillard R, Scott EM, Hermens DF. Manipulating the sleep-wake cycle and circadian rhythms to improve clinical management of major depression. BMC Medicine. 2013;11:79. DOI: 10.1186/1741-7015-11-79.
18. Healy KL, Morris AR, Liu AC. Circadian synchrony: Sleep, nutrition, and physical activity. Front. Netw. Physiol. 2021;1:732243. DOI: 10.3389/fnetp.2021.732243.

19. Rajaratnam SMW, Licamele L, Birznieks G. Delayed sleep phase disorder risk is associated with absenteeism and impaired functioning. Sleep Health. 2015;1(2):121–127. DOI: 10.1016/ j.sleh. 2015.03.001.
20. Sack RL, Auckley D, Auger RR, Carskadon MA, Wright Jr KP, Vitiello MV, Zhdanova IV. Circadian rhythm sleep disorders: Part II, advanced sleep phase disorder, delayed sleep phase disorder, free-running disorder, and irregular sleep-wake rhythm. Sleep. 2007;30(11): 1484–1501. DOI: 10.1093/sleep/30.11.1484.
21. Tekieh T, Lockley SW, Robinson PA, McCloskey S, Zobaer MS, Postnova S. Modeling melanopsin-mediated effects of light on circadian phase, melatonin suppression, and subjective sleepiness. Journal of Pineal Research. 2020;69(3):e12681. DOI: 10.1111/jpi.12681.
22. Postnova S, Lockley SW, Robinson PA. Sleep propensity under forced desynchrony in a model of arousal state dynamics. Journal of Biological Rhythms. 2016;31(5):498–508. DOI: 10.1177/ 0748730416658806.
23. Dong E, Liang Z. The multi-frequency EEG rhythms modeling based on two-parameter bifurcation of neural mass model. In: 2014 IEEE International Conference on Mechatronics and Automation. 03-06 August 2014, Tianjin, China. New York: IEEE; 2014. P. 1564–1569. DOI: 10.1109/ICMA. 2014.6885933.
24. Weigenand A, Schellenberger Costa M, Victor Ngo HV, Claussen JC, Martinetz T. Characterization of K-complexes and slow wave activity in a neural mass model. PLoS Comput. Biol. 2014;10(11): e1003923. DOI: 10.1371/journal.pcbi.1003923.
25. Phillips AJK, Robinson PA. A quantitative model of sleep-wake dynamics based on the physiology of the brainstem ascending arousal system. Journal of Biological Rhythms. 2007;22(2):167–179. DOI: 10.1177/0748730406297512.
26. Phillips AJK, Czeisler CA, Klerman EB. Revisiting spontaneous internal desynchrony using a quantitative model of sleep physiology. Journal of Biological Rhythms. 2011;26(5): 441–453. DOI: 10.1177/0748730411414163.
27. St Hilaire MA, Klerman EB, Khalsa SBS, Wright Jr KP, Czeisler CA, Kronauer RE. Addition of a non-photic component to a light-based mathematical model of the human circadian pacemaker. Journal of Theoretical Biology. 2007;247(4):583–599. DOI: 10.1016/ j.jtbi.2007.04.001.
28. Berson DM. Strange vision: ganglion cells as circadian photoreceptors. Trends in Neurosciences. 2003;26(6):314–320. DOI: 10.1016/S0166-2236(03)00130-9.
29. Wong KY, Dunn FA, Graham DM, Berson DM. Synaptic influences on rat ganglion-cell photoreceptors. The Journal of Physiology. 2007;582(1):279–296. DOI: 10.1113/jphysiol. 2007.133751.
30. Kloeden PE, Platen E. Higher-order implicit strong numerical schemes for stochastic differential equations. Journal of Statistical Physics. 1992;66(1–2):283–314. DOI: 10.1007/BF01060070.
31. Khodabin M, Rostami M. Mean square numerical solution of stochastic differential equations by fourth order Runge-Kutta method and its application in the electric circuits with noise. Advances in Difference Equations. 2015;1:62. DOI: 10.1186/s13662-015-0398-6.
32. Rackauckas C, Nie Q. Adaptive methods for stochastic differential equations via natural embeddings and rejection sampling with memory. Discrete and Continuous Dynamical Systems - B. 2017;22(7): 2731–2761. DOI: 10.3934/dcdsb.2017133.
33. Pikovsky A, Rosenblum M, Kurths J. Synchronization: A Universal Concept in Nonlinear Sciences. Cambridge: Cambridge University Press; 2001. 432 p. DOI: 10.1017/CBO9780511 755743.
34. Balanov A, Janson N, Postnov D, Sosnovtseva O. Synchronization: From Simple to Complex. Berlin, Heidelberg: Springer; 2008. 426 p. DOI: 10.1007/978-3-540-72128-4.
35. Postnov DE, Balanov AG, Sosnovtseva OV, Mosekilde E. Chaotic hierarchy in high dimen-

sions. International Journal of Modern Physics B. 2000;14(24):2511–2527. DOI: 10.1142/S0217979200002296.
36. Zeitzer JM, Dijk DJ, Kronauer RE, Brown EN, Czeisler CA. Sensitivity of the human circadian pacemaker to nocturnal light: melatonin phase resetting and suppression. The Journal of Physiology. 2000;526(3):695–702. DOI: 10.1111/j.1469-7793.2000.00695.x.
37. Postnov DE, Merkulova KO, Postnova S. Desynchrony and synchronisation underpinning sleep–wake cycles. The European Physical Journal Plus. 2021;136(5):488. DOI: 10.1140/epjp/s13360-021-01491-z.